



ORIGINAL PAPER

EXPLORATION AND MINERALOGICAL ANALYSIS OF ZIRCONIUM AND TITANIUM-RICH MINERALS IN SAND FROM COX'S BAZAR BEACH, BANGLADESH

Md. Ashiqur Rahman ALIF ¹⁾*, Arijit Saha AYON ¹⁾, Harun CHOWDHURY ²⁾,
Mokhlesur RAHMAN ¹⁾, Abdul Hakim SHALIM ¹⁾, Molla ZUBAER ¹⁾,
Mohamad Faiz Bin Mohd AMIN ³⁾ and Shohel RANA ⁴⁾

¹⁾ Department of Nuclear Science & Engineering, Military Institute of Science and Technology, Mirpur Cantonment, Dhaka, 1216, Bangladesh

²⁾ School of Engineering, RMIT University, Melbourne, Australia

³⁾ Faculty of Earth Science, Universiti Malaysia Kelantan, 17600 Jeli, Kelantan, Malaysia

⁴⁾ Institute of Mining, Mineralogy and Metallurgy (IMMM), Bangladesh Council of Scientific and Industrial Research (BCSIR), Joypurhat, Bangladesh

*Corresponding author's e-mail: alifashiq@gmail.com

ARTICLE INFO**Article history:**

Received 5 August 2025

Accepted 18 November 2025

Available online 24 December 2025

Keywords:

Zircon

Ilmenite

Wave Dispersion X-ray Fluorescence

X-ray Fluorescence

Induced Roll Magnetic Separator

Electrostatic Plate Separator

Tetrabromoethane

ABSTRACT

Zirconium (Zr) and titanium (Ti) are critical elements primarily derived from the minerals zircon ($ZrSiO_4$) and ilmenite ($FeTiO_3$), respectively. Zircon, often found alongside rutile and ilmenite, is a byproduct of their extraction. The high melting point, mechanical and chemical strength, and corrosion resistance of zirconium enable its use in various applications, including ceramics, nuclear fuel rod cladding, thermal insulators, catalysts, pharmaceuticals, and electronics. Similarly, titanium, obtained from ilmenite, rutile (TiO_2), and leucocoxene, is valued for its high strength, low density, and corrosion resistance, making it essential in nuclear power plant piping, heat exchangers, and condensers. This study conducts a mineralogical analysis of the five beach sand samples collected from Cox's Bazar coastal area. All five samples were collected from the back dune to get a higher percentage of heavy minerals. The elemental composition of bulk sand is determined using Wave Dispersion X-ray Fluorescence (WDXRF) and X-ray Fluorescence (XRF). Rutile, ilmenite, zircon, magnetite, and garnet of two samples (sample L-4 and L-5) among five samples were separated using an Induced Roll Magnetic Separator (IRMS) and Electrostatic Plate Separator (ESPS). The heavy mineral concentration of those two samples was determined by using a Heavy liquid separation process where tetrabromoethane was used as a density separator. Heavy minerals concentration in L-4 and L-5 samples were 34.65 wt% (weight percentage) and 47.35 wt% (weight percentage) respectively. Each separated heavy mineral was analyzed using a portable XRF; the result indicates the heavy minerals have been separated quite effectively.

1. INTRODUCTION

Situated on the southeastern coast of Bangladesh, the pristine beaches of Cox's Bazar not only showcase the beauty of the Bay of Bengal but also contain significant mineral reserves beneath their golden sands (Zaman et al., 2009). Among these hidden treasures are minerals rich in Zirconium (Zr) and Titanium (Ti), e.g., ilmenite ($FeTiO_3$), rutile (TiO_2), zircon ($ZrSiO_4$), poised to reveal their complex geochemical and mineralogical characteristics. Besides these Zr- and Ti-rich minerals, the other valuable minerals in beach placer are magnetite, garnet, and monazite (Hasan et al., 2022; Zaman et al., 2012). These heavy minerals are found in minimal amounts in igneous and metamorphic rocks. Still, because of their relatively high specific gravity and chemical and physical resistance to weathering, they often form placer deposits in river channels or along coastlines (Akon, 2019).

Zircon is typically associated with Ti-rich minerals; although their initial concentrations depend on the parent rocks, zircon is mainly obtained as a co-product during the production of rutile and ilmenite

via placer mining (Murty et al., 2007; Suiekpayev et al., 2021). This paper discusses the implications of these minerals, with an emphasis on resource processing and assessment.

The appeal of Zr- and Ti-rich minerals extends beyond their visual allure to their considerable industrial importance. Approximately 50% of zircon, which has a high refractive index and excellent chemical and mechanical properties, is utilised extensively in ceramics (Perks and Mudd, 2021). Additionally, zirconium finds use in nuclear applications, including uranium nuclear fuel cladding and other reactor internal structures, because of its stability at high temperatures (melting point = 1850 °C) and corrosion resistance (Xu et al., 2015). Titanium's high specific strength, exceptional corrosion resistance, and biocompatibility have made it a high-performance light metal with high value uses in the petrochemical, biomedical, aerospace, and defence industries (Fang et al., 2013).

This research focuses on examining the complex chemistry and mineralogy of zircon- and titanium-rich minerals found in the beach placer deposits of Cox's

Bazar in Bangladesh. Its primary aim is to elucidate their detailed structural features and elemental composition through advanced analytical methods, providing insights into their origins and geological history. By studying the chemical and mineralogical characteristics of these minerals, the research seeks to generate valuable knowledge that extends beyond purely academic interest. The results may guide resource management strategies, encourage sustainable processing techniques, and support a balanced utilisation of these valuable minerals.

2. LITERATURE REVIEW

Zircon is a mineral commonly found in volcanic rocks and sedimentary deposits, renowned for its distinctive crystalline structure and its use in radiometric dating. Coastal sediments often contain zircon alongside heavy minerals such as ilmenite, rutile, and garnet. This review examines academic research on the occurrence of heavy minerals, including zircon, rutile, and ilmenite, in coastal environments.

Hasan et al. (2022) studied the geochemical and mineralogical features of zircon, rutile, and ilmenite from Cox's Bazar beach sand, emphasising their economic worth and possible beneficiation methods. Their research employed X-ray fluorescence (XRF), X-ray diffraction (XRD), scanning electron microscopy (SEM), and electron probe microanalysis (EPMA) to examine mineral diversity and origin. They observed zircon mainly in the 125 to 63 μm size range, with ilmenite and rutile present across all sizes. However, a more comprehensive economic analysis could enhance the findings (Hasan et al., 2022). This research evaluates the economic significance of heavy mineral sands for Bangladesh, focusing on ilmenite, zircon, and rutile as the key minerals. Systematic sampling, heavy liquid separation techniques (Bromoform and Methylene iodide), and magnetic separation procedures were utilised. Coastal regions and rivers were also crucial for mineral exploration, revealing an average of 23 % of heavy minerals available. The weight percentages of these minerals were ilmenite (26.03 %), zircon (4.20 %), and rutile (2.04 %). Nonetheless, further research is necessary to improve feasibility and address environmental policies (Eunuse Akon, 2019).

The study focused on analysing the distribution of heavy minerals, mineral composition, and trace element concentrations in the sandy beaches of Sonadia Island, Cox's Bazar district, Bangladesh. Fourteen samples were collected from a depth of 1 metre across the research area, each weighing approximately 5 to 10 kg. Radioactivity in the area was measured using a portable gamma-ray spectrometer. In the heavy liquid separation process, "Bromoform" was used to determine the weight percentage of heavy minerals, with grain counting employed for accuracy. The findings revealed weight percentages of various heavy minerals, including garnet (33.24 % to 62.43 %), ilmenite (21.39 % to

56.27 %), and magnetite (0.5 % to 3.74 %), among others. Elemental analysis using XRF showed average concentrations of elements such as Zr (198.75 ppm), Fe (15,127 ppm), and Ti (1,598 ppm). The amount of heavy minerals detected is not significant. Radiation levels in the study area ranged from 24 to 170 counts per second (cps). The study concluded that Sonadia Island contains a small quantity of heavy minerals. The paper could further explore the implications of these findings for resource management and environmental conservation, particularly in the context of coastal development pressures (Kabir et al., 2018).

Neutron activation analysis (NAA) measured uranium and thorium levels in zircon from Cox's Bazar, revealing significant concentrations that must be considered during mining operations. The results carry important implications for environmental management and public health. The presence of radioactive elements in zircon could pose risks to mine workers and nearby communities, mainly if not adequately managed. The authors emphasise the need for further research to understand the long-term impacts of these elements on human health and the environment, which is a vital issue that demands attention. (Zaman et al., 2016).

Mitra et al. (1992) characterized the mineralogical and chemical nature of opaque minerals present in Cox's Bazar beach sand, providing the geological background — i.e., ilmenite, hematite, and magnetite are the main minerals, while semi-opaque minerals make up about 15-30 % of the heavy mineral content in the sediments. Researchers employ methods such as electron microprobe analysis, magnetic separation, and sieving to determine the content of heavy minerals. However, the study has several limitations. The sampling technique is not sufficiently detailed; samples were collected from shallow depths of 10-30 cm. Furthermore, conclusions regarding mineral sources are limited by reliance on individual geochemical techniques. A more comprehensive understanding of the sedimentary processes and mineral provenance of Cox's Bazar sands would have benefited significantly from clearer sampling procedures and standardised analytical protocols (Mitra et al., 1992).

The research article titled "Heavy Mineral Assemblages of the Beach Sands of Kuakata, Southern Bangladesh" thoroughly examined the heavy minerals present in Kuakata beach sand. Researchers collected a total of 17 samples, of which 5 were selected for detailed heavy mineral analysis. Heavy liquid separation was used to isolate the heavy minerals, which were then examined under a polarising microscope. Each mineral was identified based on its unique properties, providing insights into its origins, such as crystalline rocks. The authors presented the findings clearly and informatively. However, the study has limitations: it does not explain why only 5 samples out of 17 were chosen, and it mainly focused on grain percentages without considering variations in grain

Table 1 Sampling description at Cox's Bazar coastal area.

Sample ID	Longitude	Latitude	Depth (cm)
L-1	91.9782	21.4199	90
L-2	91.9791	21.4193	90
L-3	91.9781	21.4203	90
L-4	91.9641	21.4357	100
L-5	91.9602	21.4408	100

size, which can influence mineral distribution and hydrodynamic sorting (Bari et al., 2011).

The study included flowcharts for extracting heavy minerals from the Brahmagiri Lean Grade Beach Sand Deposit. It was the first time that individual heavy minerals, recognised for industrial use, were recovered. Spiral concentrators achieved a recovery of 98 % by weight of the total heavy minerals. The process produced high-grade mineral concentrates: ilmenite (30.2 % recovery, 98.1 % purity, 92.6 % yield), rutile (0.9 %, 98.8 %, 74.1 %), garnet (27.9 %, 97.4 %, 94.1 %), zircon (0.6 %, 98.86 %, 82.3 %), and sillimanite (27.2 %, 98.7 %, 84.6 %). Economic feasibility was confirmed through process flow sheets with mass balance analysis (Singh et al., 2023).

3. METHODOLOGY

3.1. FIELD INQUIRY

In the current study, five beach sand samples were collected from different locations along the Cox's Bazar coastline using a hand auger. The samples were labelled as L(location) with unique numerical identifiers. Samples L1, L2, L3, L4, and L5 were taken from Kolatoli Beach, the area between Sugandha and Kolatoli Beach, Sugondha Beach, Kobita Chottor, and Ujjal Beach, respectively. The sampling locations and depths are listed in Table 1.

Coordinates (latitude and longitude) for each of the five sampling sites were determined using a Global Positioning System (GPS). For samples L1, L2, and L3, sands were collected at approximately 90 cm below the surface with a hand auger. For L-4 and L-5, samples were collected approximately 1 meter below the surface. Figure 1 illustrates the locations in Cox's Bazar, a coastal area in Bangladesh, with the sites marked using their coordinates. A GIS software was employed to create this map.

3.2. ELEMENTAL ANALYSIS

After drying and pelleting the sample preparation, the samples were loaded into the wavelength-dispersive X-ray fluorescence (WDXRF) equipment. When analysing samples with XRF, they were not pelletised. The elemental composition of the samples was identified using WDXRF spectroscopy and a portable XRF device. Figure 2 shows the detailed technique used in our current study.

X-ray fluorescence (XRF) is a proper analytical technique for determining the elemental composition of bulk materials due to its wide linear range, sensitivity, accuracy, and precision (Singh et al.,

2020). The atom returns to a state where outer electrons occupy shells by emitting X-ray fluorescence radiation. The energy of the relevant electronic levels (shown by the $K\alpha$ and $K\beta$ lines in Figure 3) determines the energy of the emitted X-ray photon (fluorescence), which depends on the properties of the nucleus (Alter, 2019).

The WDXRF process follows Bragg's law. According to this law, constructive interference occurs when an incident X-ray beam with wavelength " λ " interacts with a crystal surface at an angle " q ." If the crystal has atomic lattice layers separated by a distance " d ," also called the interplanar spacing, the diffracted X-ray beam will be emitted from the crystal at an angle " q " if the condition $n\lambda = 2d \sin q$ is met (Fig. 4), where " n " is an integer (SERC, 2007).

3.3. HEAVY LIQUID SEPARATION

Heavy liquid separation was carried out on samples L4 and L5. Samples from locations 4 (L-4) and 5 (L-5) were selected for this process because they were collected from the old beach. An old beach contains more minerals than a new beach because it has had more time to accumulate them. Heavier minerals, such as zircon and ilmenite, settle and become concentrated over time. Meanwhile, lighter minerals are washed away by waves (Karikalan et al., 2020). Older beaches can also stabilise and retain minerals, while newer beaches are constantly changing and may not have accumulated as many minerals yet.

Heavy minerals were separated to determine the proportion of the heavy fraction in the unprocessed sand. The study used tetrabromoethane ($\text{Br}_2\text{CHCHBr}_2$, density 2.89 g/cm^3) as a density separator to effectively isolate the heavier components. Minerals with a specific gravity greater than that of tetrabromoethane are classified as heavy minerals. First, acid treatment with HCl and H_2O_2 was applied to remove carbonate and organic matter, achieving this goal. A 20-gram sample of unprocessed sand from locations 4 and 5 was carefully added to a wide-mouthed separating funnel containing 100-150 millilitres of tetrabromoethane, with continuous mixing. The funnel, equipped with a stopcock of a bore larger than its inner diameter, was used. The minerals floating in the tetrabromoethane were agitated, and the funnel was left undisturbed until all the heavier minerals settled. The heavy minerals and a small amount of tetrabromoethane were then transferred from the bottom of the funnel into a filter funnel with filter paper. The heavy minerals on the

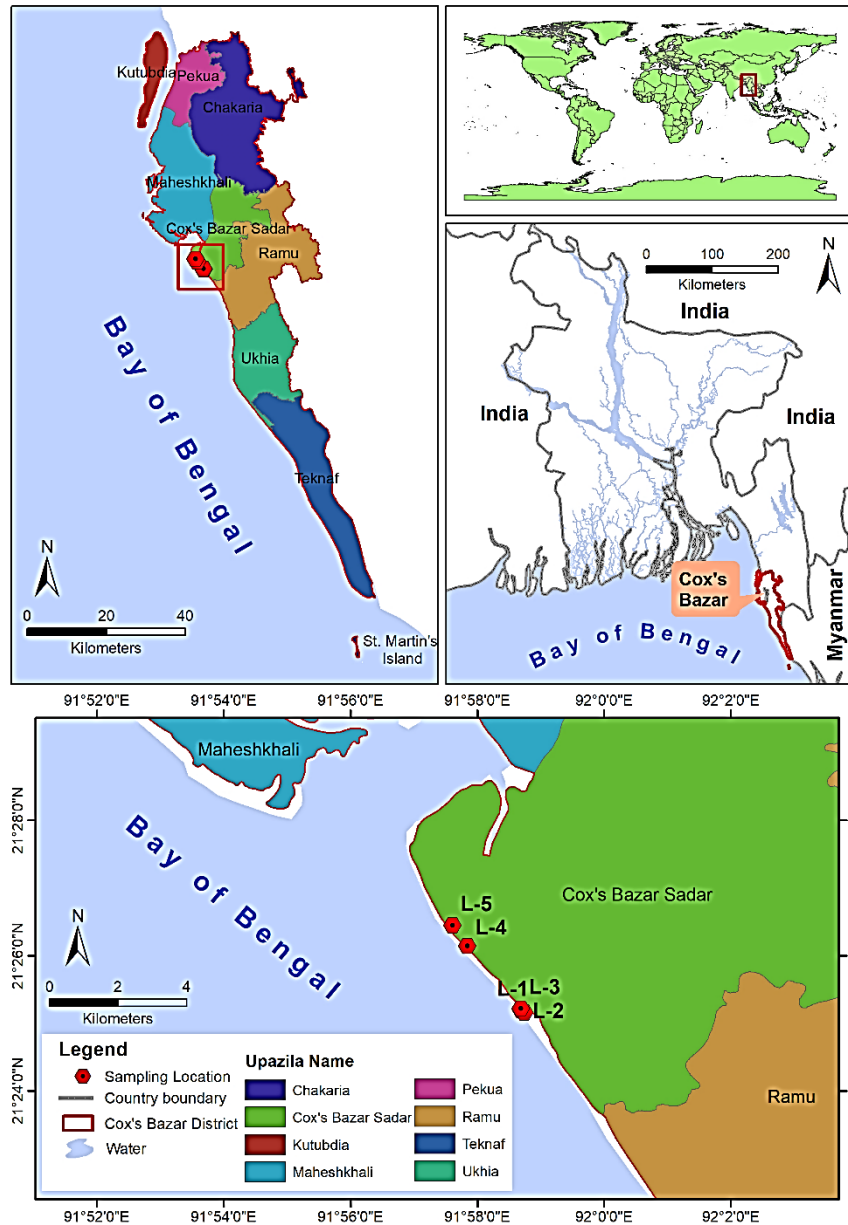


Fig. 1 Location map of the study area.

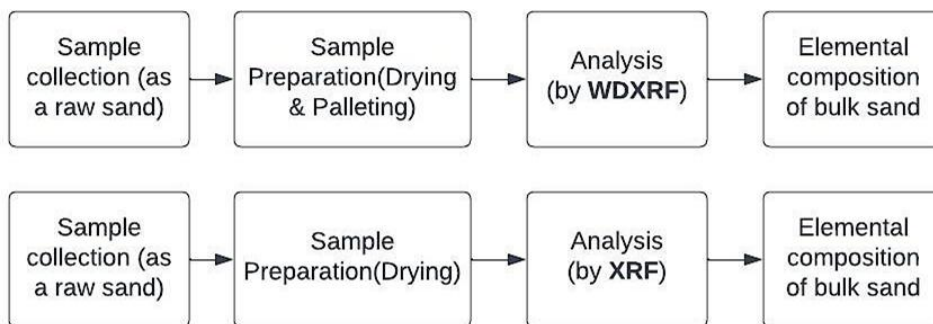


Fig. 2 Determination of elemental composition of bulk sand by WDXRF and XRF. X-ray fluorescence (XRF), is a valuable analytical method for determining the elemental makeup of bulk materials because of its dynamic linear range, sensitivity, accuracy, and precision (Singh et al., 2020). The atom returns to a state where outer electrons occupy shells by releasing X-ray fluorescence radiation. The energy of the relevant electronic levels (shown by the $K\alpha$ and $K\beta$ lines in Fig. 3) determines the energy of the generated X-ray photon (fluorescence), which in turn depends on the properties of the nucleus (Alter, 2019).

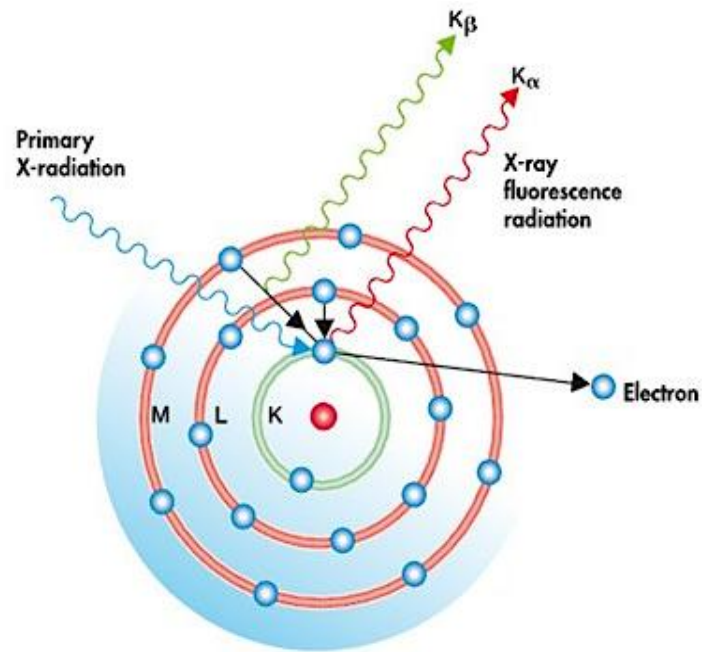


Fig. 3 Working principle of XRF (Alter, 2019).

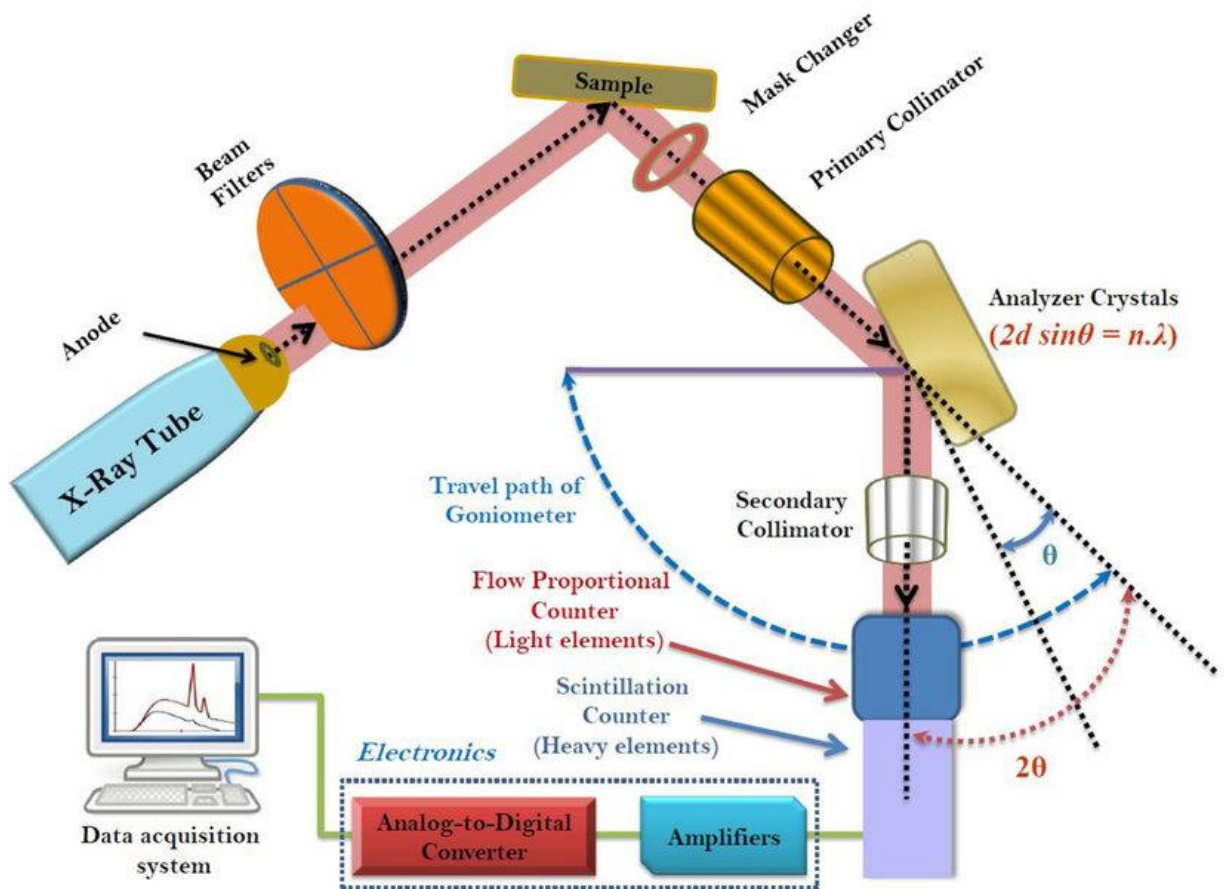


Fig. 4 WDXRF diagram (Singh et al., 2020).

filter paper were cleansed, and tetrabromoethane was removed using acetone. Grain-count studies of the heavy minerals were performed on the fine-to-fine sand fraction (63-500 μm).

3.4. MICROSCOPIC STUDY OF THE PREPARED SAMPLE

Mineralogical analysis of the sand samples was conducted using a Nikon SMZ745T (Japan-made) stereomicroscope. The minerals were identified, quantified, and measured along ten to fifteen evenly spaced traverses. Each mineral, whether opaque (such as ilmenite, rutile, and garnet) or non-opaque (such as zircon and kyanite), was counted by examining at least 200 grains through the ribbon method (Mange and Maurer, 1992). The minerals were carefully analysed for their colour, crystal structure, size, inclusions, and relative abundance through microscopic grain counting in view slices. Photographs were captured with a DeltaPix camera connected to the microscope. The weight percentage of the individual heavy minerals can be calculated using equation (1).

$$\text{wt}\% = 100(a * b) / (a * b) \% \quad (1)$$

Where wt% is the weight percentage of the individual heavy minerals, a is the specific gravity of a particular mineral of interest, and b is the number of grains of a specific mineral of interest.

3.5. DRY SEPARATION

Our aim in this procedure is to extract zircon, rutile, and ilmenite from materials obtained from the coastal region of Cox's Bazar. L-4 and L-5 were selected for the process. As our sample size was small (approximately 3 kg), separation using a shaking table was not feasible. Therefore, the bulk samples were directly segregated into magnetic and non-magnetic fractions using an induced roll magnetic separator (IRMS). Subsequently, a hand magnet was used to separate the high magnetic fraction (magnetite) from the low magnetic fraction (ilmenite). Afterwards, the non-magnetic fractions were further divided into low-magnetic fractions and non-magnetic fractions. Conductor and non-conductor fractions were separated from the low magnetic and non-magnetic fractions using an electrostatic plate separator (ESPS). The low magnetic fractions were used to isolate ilmenite and garnet, while the non-magnetic fractions were used to isolate rutile and zircon. Ilmenite and rutile are classified as conductive fractions, whereas garnet and zircon are categorised as non-conductive fractions. This process is illustrated in a flowchart in Figure 5.

4. RESULT AND DISCUSSION

4.1. ELEMENTAL COMPOSITION BEFORE SEPARATION

Tables 2 and 3 display the elemental composition of samples collected from various locations along the Cox's Bazar coast. Initially, samples from locations 1, 2, and 3 were analysed using WDXRF. During

WDXRF analysis, a vacuum is created, and the sample is placed within it. Since the samples consisted of raw sand, the sand particles could move freely in the vacuum if a proper binder was not used. This movement could potentially damage the WDXRF equipment, leading to inaccurate results. Therefore, for subsequent analyses, a portable XRF device was used.

When WDXRF was used, the percentage of Zr ranged from 0.67 to 2.90 % across all three samples analysed. Concerning Ti, the sample labelled as L-1 showed the highest percentage (5.44 %), while the sample identified as L-2 had the lowest percentage (1.56 %).

When the samples were analysed using XRF, the percentage of Zr ranged from 0.141 % to 1.898 %, and for Ti, it ranged from 1.17 % to 5.06 %. Tables 2 and 3 show that the elemental composition of all five samples was determined using a portable XRF. The results of L-1, L-2, and L-3 differed slightly from WDXRF due to some limitations of the portable XRF method. The percentages of Zr and Ti in samples collected from different locations are shown in Figures 6 and 7. In both figures, it is evident that the Ti percentage exceeds the Zr percentage.

4.2. HEAVY LIQUID SEPARATION

Heavy and light minerals were separated using the heavy liquid separation process. Data on the distribution of these minerals in both bulk samples are shown in Table 4.

The average heavy mineral content was 34.65 % for L-4, and for L-5, it was 47.35 %. It was also observed that light minerals were present in higher amounts than heavy minerals. The average percentages of light minerals were 65.35 % and 52.61 % in L4 and L5, respectively.

Figure 8 shows a photomicrograph highlighting rutile, opaque minerals, garnet, and zircon. This photomicrograph was captured by analysing the sample under a Nikon SMZ745T (origin: Japan) stereoscopic microscope.

The analysis of samples from locations 4 and 5 showed that opaque minerals, especially ilmenite and magnetite, had the highest levels, as both appeared blackish under the microscope and were hard to distinguish, which led to their classification as opaque. In Table 5, zircon concentration was about 2 wt% and rutile were around 1.5 wt% in samples from location 4. The amounts of other heavy minerals, such as garnet, tourmaline, monazite, kyanite, and sillimanite, were approximately 6.5 wt%, 0.4 wt%, 2.9 wt%, 0.8 wt%, and 1.7 wt%, respectively, found in L-4.

The zircon and rutile concentrations were 2.6 wt% and 1.2 wt%, respectively, as shown in Table 6.

The concentrations of other heavy minerals such as garnet, tourmaline, monazite, kyanite, and sillimanite were approximately 4.8 wt%, 0.3 wt%, 2.7 wt%, 0.9 wt%, and 1.6 wt%, respectively, found in L-5.

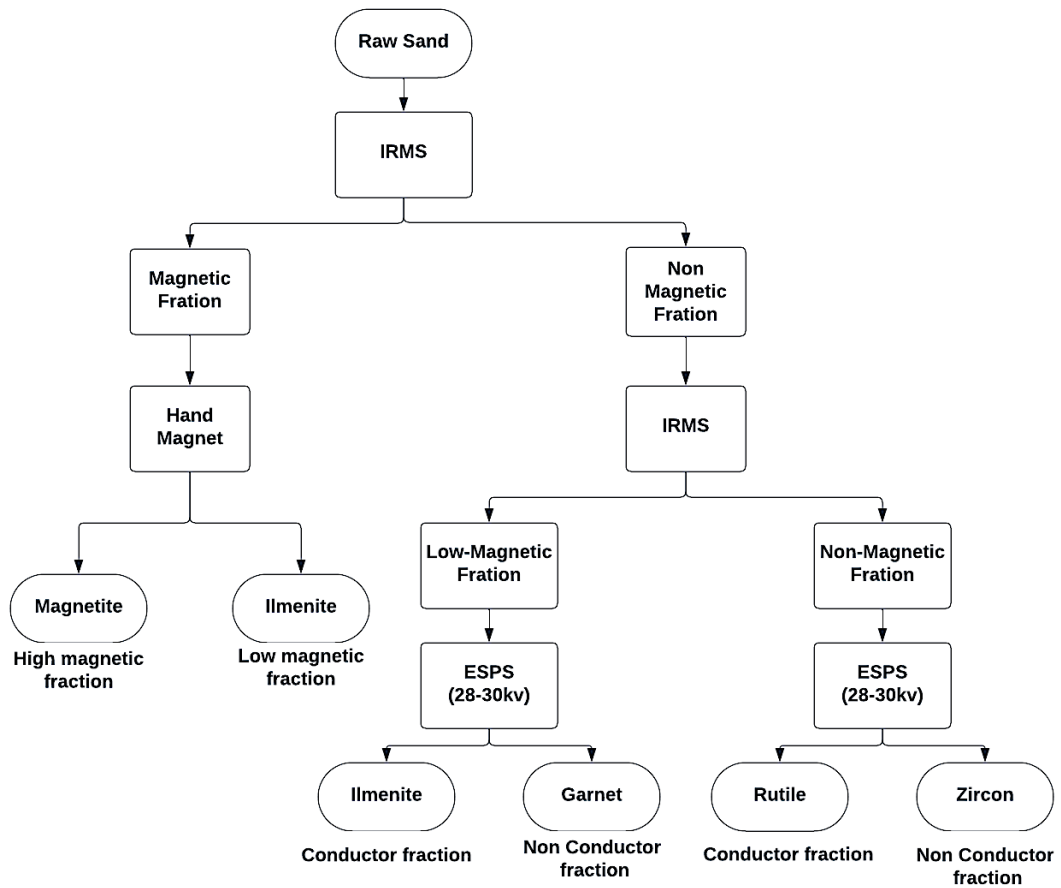


Fig. 5 Heavy minerals separation process.

Table 2 The elemental composition of bulk sand of the three samples using WDXRF (Zr and Ti).

Analyte	L-1 (%)	L-2 (%)	L-3 (%)
Zr	1.32	0.67	2.90
Ti	5.44	1.56	4.15

Table 3 The elemental composition of bulk sand of the five samples using portable XRF (Zr and Ti).

Analyte	L-1 (%)	L-2 (%)	L-3 (%)	L-4 (%)	L-5 (%)
Zr	1.898	0.141	0.181	0.44	0.696
Ti	5.06	1.17	2.16	2.88	3.95

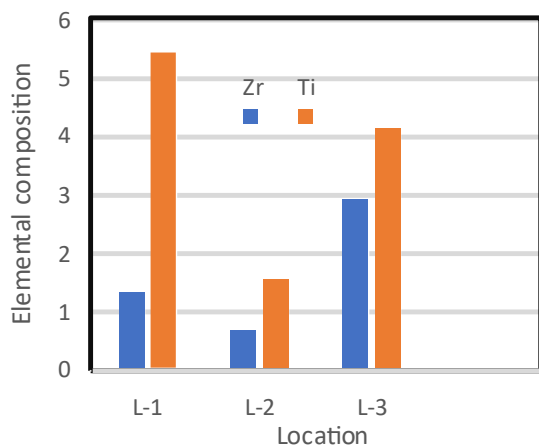


Fig. 6 Elemental composition comparison among three samples (L-1, L-2, L-3) (using WDXRF).

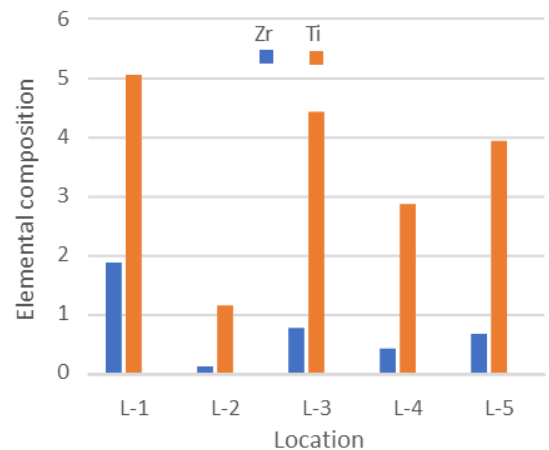
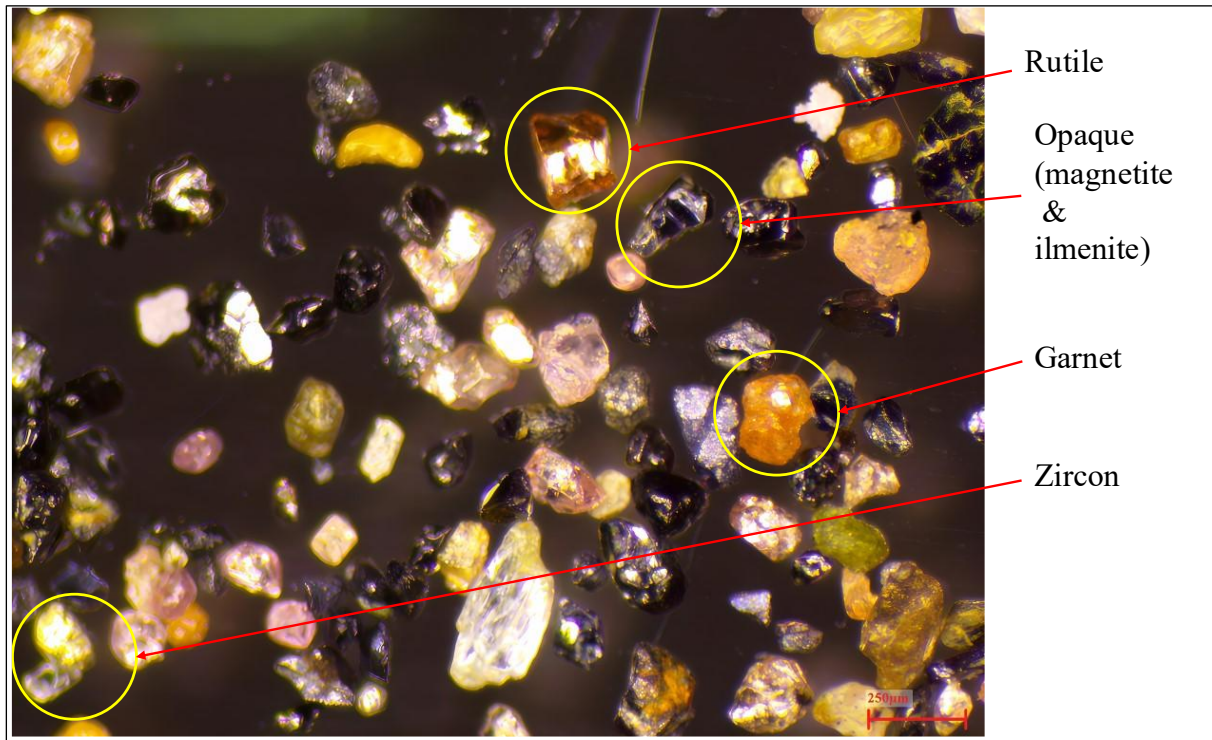


Fig. 7 Elemental composition comparison among five samples (L-1, L-2, L-3, L-4 and L-5) (using XRF).

Table 4 Data for heavy and light minerals distribution in both bulk samples.

Sample ID	Sample	Heavy (%)	Average (%)	Light (%)	Average (%)
L-4	A	34.58	34.65	65.48	65.35
	B	34.72		65.22	
L-5	A	49.25	47.35	50.77	52.61
	B	45.46		54.45	

**Fig. 8** Photomicrographs of rutile, opaque, garnet and zircon.**Table 5** Heavy mineral concentration in wt% of L-4 sample (Opaque: Ilmenite and magnetite).

Heavy mineral	Grain number	Specific Gravity (gm/cc)	Weight (gm)	Weight percentage, wt%	Weight percentage in Heavy, wt%
Opaque	421	9.9	4168.0	84.2	29.2
Zircon	21	4.6	96.6	2.0	0.7
Rutile	18	4.2	75.6	1.5	0.5
Garnet	81	4.0	324.0	6.5	2.3
Tourmaline	6	3.0	18.0	0.4	0.1
Monazite	30	4.8	144.0	2.9	1.0
Kyanite	11	3.5	38.5	0.8	0.3
Sillimanite	26	3.2	83.2	1.7	0.6
Total			4948.0		

4.3. DRY SEPARATION PROCESS

Heavy minerals were separated using a hand magnet, an induced roll magnetic separator, and an electrostatic plate separator. Ilmenite, garnet, zircon, and rutile were finally obtained from the electrostatic plate separator. Following dry separation, the percentage of each heavy mineral is shown in Table 7.

The fraction of each heavy mineral was determined by its weight. The samples with the highest percentage of the mag mix were L-4 and L-5. There

was 0.47 percent rutile in L-5. However, rutile was absent from L-4 due to difficulties in isolating it. In L-4, the percentages of heavy minerals zircon mix, ilmenite, garnet, magnetite, and mag mix were 1.56 %, 9.37 %, 7.50 %, 5.31 %, and 29.37 %, respectively. Conversely, in L-5, the percentages of heavy minerals were 1.41 %, 12 %, 20.47%, 7.65 %, and 41.41 % for zircon mix, ilmenite, garnet, magnetite, and mag mix, respectively.

Table 6 Heavy mineral concentration in wt% of L-5 sample (opaque: Ilmenite and magnetite).

Heavy mineral	Grain number	Specific Gravity (gm/cc)	Weight (gm)	Weight percentage, wt% (%)	Weight percentage in Heavy, wt% (%)
Opaque	416	9.9	4118.4	85.7950	40.6238
Zircon	27	4.6	124.2	2.5873	1.22511
Rutile	14	4.2	58.8	1.2249	0.58
Garnet	58	4	232	4.8330	2.28844
Tourmaline	5	3	15	0.3125	0.14796
Monazite	27	4.8	129.6	2.6998	1.27837
Kyanite	13	3.5	45.5	0.9479	0.44881
Sillimanite	24	3.2	76.8	1.5999	0.75755
Total			4800.3		

Table 7 Heavy mineral percentage after dry separation (n.d.= not detected).

Heavy minerals	Location	
	L-4 (%)	L-5 (%)
Zircon mix	1.56	1.41
Rutile mix	n.d.	0.47
Ilmenite	9.37	12
Garnet	7.5	20.47
Magnetite	5.31	7.65
Mag mix	29.37	41.41

Using portable XRF, the separated minerals were analysed, revealing Zr (48.83 %), Ti (33.73 %), and Fe (93.42 %) as the main elemental components of zircon, rutile, and magnetite, respectively. Ti (20.60%) and Fe (69.88 %) were identified in the analysis of ilmenite. From the analysis of garnet, Fe (66.80 %), Al (9.97 %), and Si (17.47 %) were detected. The separation process was successful, as indicated by the higher percentages of Zr in zircon, Ti in ilmenite, and Fe in magnetite, along with the levels of Ti and Fe in ilmenite and Fe, Al, and Si in garnet.

The microstructures of individual heavy minerals were examined using a Nikon SMZ745T stereoscopic microscope. Zircon grains were observed as short prismatic crystals with euhedral to subhedral forms and edges that range from angular to rounded and broken. They vary in colour from white to yellowish brown, featuring a black border (Fig. 9a). Although colour alone is insufficient for identification, noting the colour can help verify other characteristics (Bari et al., 2011). 1.56 % and 1.41 % of zircon were obtained from the heavy mineral concentrates of L-4 and L-5, respectively.

The microstructure of rutile is shown in Figure 9(b). Rutile was identified by its brownish, honey-yellow, or reddish brick colour, and its euhedral to subhedral short prismatic form (Bari et al., 2011). Rutile proved difficult to isolate, which is why it was undetectable in L-4 and accounted for only 0.47 % of the heavy minerals concentrate in L-5.

Garnet grains are generally colourless, although some pale pinkish grains are also present (Fig. 9c). Their high relief and display of pitted, corroded surface marks, along with an isotropic characteristic, distinguish them (Bari et al., 2011). In the heavy

mineral concentrates, garnet was found in concentrations of 7.5 % in sample L-4 and 20.47 % in sample L-5.

Ilmenite's microstructure is illustrated in Figure 9(d). Ilmenite appears as brownish to iron-black in colour. The crystals can be partially identified as rhombohedral (Geologyscience, 2023a). The heavy mineral concentrates of L-4 and L-5 contained 9.37 % and 12 % ilmenite, respectively.

When observed under a microscope, magnetite, a common iron oxide mineral, exhibits distinctive features. Magnetite is opaque and appears black and grey with a brownish tint in reflected light. It typically forms as octahedral crystals, although it can sometimes be twinned (Geologyscience, 2023b). The microstructure of magnetite is shown in Figure 9(e). 5.31 % of magnetite was extracted from the heavy minerals' concentration of L-4, while 7.65 % was recovered from L-5.

The study focused on analysing the distribution of heavy minerals and the elemental composition of beach sands in Cox's Bazar. The research aimed to understand the geological features and resource extraction potential of Zr- and Ti- rich minerals through field investigation and mineral separation techniques. In this study, approximately 3 kg of samples were collected from location 4 and location 5, which resulted in an outcome. The amount was insufficient to operate the shaking table. The light minerals could not be separated, leading them to behave as undesired impurities in the zircon and rutile mixture. Quartz, a light mineral, was also present in the heavy mineral fraction after heavy liquid separation. A larger bulk sample will provide more accurate results.

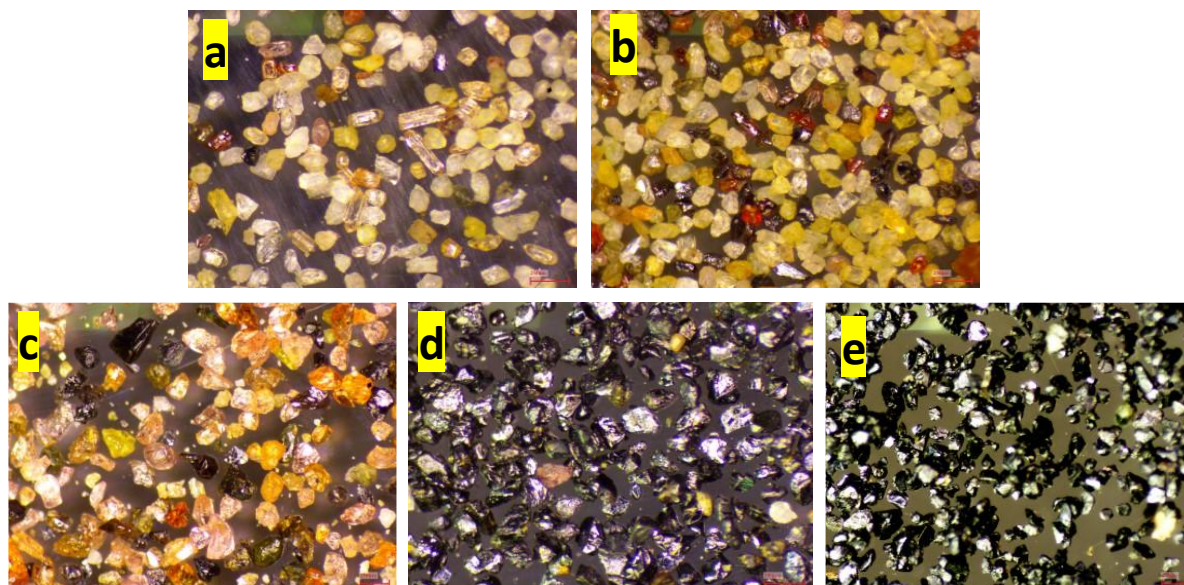


Fig. 9 Photomicrographs of (a) zircon mix, (b) rutile mix, (c) garnet mix, (d) ilmenite, (e) magnetite.

Table 8 wt% comparison of heavy minerals in sample location L-4 with recent studies.

Heavy minerals	Our sample(L4)	Sample from Jhawtola Beach (Zaman et al., 2022)
Zircon	1.95	3.54
Rutile	1.53	3.21

Table 9 wt% comparison of heavy minerals in sample location L-5 with recent studies.

Heavy minerals	Our sample(L5)	Sample from Jhawtola Beach (Zaman et al., 2022)
Zircon	2.58	3.54
Rutile	1.22	3.21

4.4. wt% COMPARISON WITH RECENT RESEARCH

Tables 8 and 9 compare the wt% of major heavy minerals obtained in this study with previously published data. This comparison helps illustrate mineralogical similarities, variations in concentration, and the relative resource potential of the Cox's Bazar beach deposits.

4.5. ECONOMIC AND PRACTICAL VIABILITY OF PHYSICAL SEPARATION METHODS OF DRY SEPARATION OF HEAVY MINERALS

The total cost of dry separation of L-4 and L-5 is 46,400 takas, which is approximately \$ 380. The breakdown of the cost is given in Tables 10 and 11.

The total cost of dry separation is \$ 380. In our laboratory-scale studies, this expense was considered economically viable due to the reduced processing time, elimination of reagent costs, and scalability benefits it offered compared to conventional methods. Physical separation methods are also environmentally friendly, widely used, and effective for preliminary

heavy mineral concentration. While the cost-benefit analysis would need to be thorough for commercial application, our studies aim to demonstrate the viability and potential of physical methods in heavy mineral separation.

5. CONCLUSIONS

A study conducted in the Cox's Bazar Coastal Area of Bangladesh provides valuable insights into the mineral composition and resource potential of the region. The research emphasises the mineral composition, extraction sources, and analysis techniques used, including Wave Dispersion X-ray Fluorescence (WDXRF), X-ray Fluorescence (XRF), and separation methods such as magnetic and electrostatic separation. The findings highlight significant heavy mineral contents in samples L-4 and L-5, with concentrations of 34.65 wt% and 47.35 wt%, respectively, demonstrating the potential for mineral extraction and application. The study highlights the significance of mineral properties, such as durability

Table 10 Cost of dry separation of L-4 (IMMM et al., 2025).

Instrument	Testing Cost per amount (taka/kg)	Sample amount (kg) tested	Cost (Taka)
ESPS	20,000.00	0.236	4720.00
IRMS	5,000.00	3.000	15,000.00
Total cost			19,720.00

Table 11 Cost of dry separation of L-5 (IMMM et al., 2025).

Instrument	Testing Cost per amount (taka/kg)	Sample amount (kg) tested	Cost (Taka)
ESPS	20,000.00	0.584	11,680.00
IRMS	5,000.00	3.000	15,000.00
Total cost			26,680.00

and corrosion resistance, for various industrial applications, including ceramics, nuclear fuel cladding, and construction.

Future research will expand on these conclusions by collecting additional samples to increase zircon yield. Microstructural analysis using Scanning Electron Microscopy (SEM) will enhance understanding of mineral characteristics. Moreover, zircon samples will undergo irradiation in a 3 MW TRIGA Mark II Research Reactor at BAEC, followed by Neutron Activation Analysis (NAA), with gamma-ray emissions measured via HPGe detectors. The activity concentrations of uranium and thorium will be quantified based on gamma-ray peaks at 277 keV and 312 keV, respectively, as referenced by Zaman et al. (2016).

ACKNOWLEDGEMENT

Authors express their sincere gratitude to ABSCUBE Engineering & Education Services Pty Ltd (Australia) for their editorial support, which contributed to enhancing the quality of this article.

FUNDING

This project was funded by the Department of Nuclear Science & Engineering, Military Institute of Science and Technology (Bangladesh) and

ABSCUBE Engineering & Education Services Pty Ltd (Australia).

AVAILABILITY OF DATA AND MATERIALS

The data backing the findings of this study can be obtained from the corresponding author on reasonable request.

COMPETING INTERESTS

The authors declare that they have no competing interests.

DECLARATIONS:

(a) Ethics and consent: Not applicable.

REFERENCES

- Akon, E.: 2019, Mineralogy, geochemistry and economic potentialities of heavy mineral sand resources of Bangladesh. *Journal of Nepal Geological Society*, 59, 1–8. DOI: 10.3126/jngs.v59i0.58589
- Alter: 2019, XRF: X-Ray Fluorescence Spectroscopy | Hi Rel Parts. Available at: <https://wpo-altertechnology.com/xrf-x-ray-fluorescence-spectroscopy-hi-rel-parts/>
- Bari, Z., Rajib, M. and Ameen, S.M.M.: 2011, Heavy mineral assemblages of the beach sands of Kuakata, Southern Bangladesh. *Jahangirnagar University Journal of Science*, 34, 2, 143–158.
- Fang, Z.Z., Middlemas, S., Guo, J. and Fan, P.: 2013, A new, energy-efficient chemical pathway for extracting Ti metal from Ti minerals. *Journal of the American Chemical Society*, 135(49), 18248–18251. DOI: 10.1021/ja408118x
- Geologyscience: 2023a, Ilmenite. Available at: <https://geologyscience.com/minerals/ilmenite/>
- Geologyscience: 2023b, Magnetite. Available at: <https://geologyscience.com/minerals/magnetite/>
- Hasan, A.S.M.M., Hossain, I., Rahman, M.A., Zaman, M.N., Biswas, P.K. and Alam, M.S.: 2022, Chemistry and mineralogy of Zr- and Ti-rich minerals sourced from Cox's Bazar beach placer deposits, Bangladesh: Implication of resources processing and evaluation. *Ore Geology Reviews*, 141, 104687. DOI: 10.1016/j.oregeorev.2021.104687
- IMMM: 2025, Analytical Service. Available at: <https://immm.bcsir.gov.bd/site/page/5160584a-02fc-4889-86e2-d74eb46fdde4/Analytical-Service>
- Kabir, M.Z., Deeba, F., Rasul, M.G., Majumder, R.K., Khalil, M.I. and Islam, M.S.: 2018, Heavy mineral distribution and geochemical studies of coastal sediments at Sonadia Island, Bangladesh. *Nuclear Science and Applications*, 27(1–2), 1–5. DOI: 10.3329/nsa.v27i1-2.53775
- Karikalan, R., Sathasivam, R. and Rakkiannan, S.: 2020, XRD analysis in Gundar river estuary and beach sediments of Mookaiyur area, Ramanathapuram District, South India. *International Journal of Engineering Research and Technology*, 9, 4. DOI: 10.17577/ijert.9(4).341-344
- Mange, M.A. and Maurer, H.F.W.: 1992, Heavy Minerals in Colour. Chapman and Hall, London. DOI: 10.1007/978-94-011-2308-2
- Mitra, S., Ahmed, S.S. and Moon, H.-S.: 1992, Mineralogy and chemistry of the opaques of Cox's Bazar beach sands and the oxygen fugacity of their provenance. *Sedimentary Geology*, 77, 3-4, 235–247. DOI: 10.1016/0037-0738(92)90129

- Murty, V.G.K., Upadhyay, R. and Asokan, S.: 2007, Recovery of zircon from Sattankulam deposit in India—problems and prospects. In: The 6th International Heavy Minerals Conference “Back to Basics”, South African Institute of Mining and Metallurgy, 69–74.
- Perks, C. and Mudd, G.: 2021, Soft rocks, hard rocks: The world’s resources and reserves of Ti and Zr and associated critical minerals. *International Geology Review*, 1–22.
DOI: 10.1080/00206814.2021.1904294
- SERC: 2007, X-ray reflection in accordance with Bragg’s Law. Available at:
https://serc.carleton.edu/research_education/geochem_sheets/BraggsLaw.html
- Singh, D., Basu, S., Mishra, B.R. and Rao, R.B.: 2023, Development of flow sheets to recover critical minerals from Brahmagiri lean-grade beach sand deposit. *Journal of The Institution of Engineers (India): Series D*. DOI: 10.1007/s40033-023-00514-6.
- Singh, V.K., Jaswal, B.J., Sharma, J. and Rai, P.K.: 2020, Analysis of stones formed in the human gall bladder and kidney using advanced spectroscopic techniques. *Biophysical Reviews*.
DOI: 10.1007/s12551-020-00697-2
- Suiekpayev, Y.S., Sapargaliyev, Y.M., Dolgoplova, A.V., Pirajno, F., Seltmann, R., Khromykh, S.V., Bekenova, G.K., Kotler, P.D., Kravchenko, M.M. and Azelkhanov, A.Z.: 2021, Mineralogy, geochemistry and U-Pb zircon age of the Karaotkel Ti-Zr placer deposit, Eastern Kazakhstan. *Ore Geology Reviews*, 131, 104015. DOI: 10.1016/j.oregeorev.2021.104015
- Xu, L., Xiao, Y., van Sandwijk, A., Xu, Q. and Yang, Y.: 2015, Production of nuclear grade zirconium: A review. *Journal of Nuclear Materials*, 466, 21–28.
DOI: 10.1016/j.jnucmat.2015.07.010
- Zaman, M.M., Deebea, F., Kabir, M.Z., Rajib, M. and Rana, S.M.: 2009, Finding a new heavy mineral deposit and its mineralogical composition at Sonarpara, Cox’s Bazar. *Journal of NOAMI*, 26, 17–30.
- Zaman, M.M., Rajib, M., Kabir, M.Z., Deebea, F., Rana, S.M., Hossain, S.M., Latif, S.A. and Rasul, M.G.: 2016, Presence of uranium and thorium in zircon assemblages separated from beach sands of Cox’s Bazar, Bangladesh. *Journal of Science, Technology and Environmental Informatics*, 3, 1, 161–168.
DOI: 10.18801/jstei.030116.18
- Zaman, M., Schubert, M. and Antao, S.M.: 2012, Elevated radionuclide concentrations in heavy mineral-rich beach sands in the Cox’s Bazar region, Bangladesh and related possible radiological effects. *Isotopes in Environmental and Health Studies*, 48(4), 512–525.
DOI: 10.1080/10256016.2012.696542